The Retina in Alzheimer's Disease: Histomorphometric Analysis of an Ophthalmologic Biomarker

Samuel Asanad,[1,2] Fred N. Ross-Cisneros,[1] Marco Nassisi,[1] Ernesto Barron,[1] Rustum Karanjia,[1–4] and Alfredo A. Sadun[1,2]

[1]Doheny Eye Institute, Los Angeles, California, United States
[2]Department of Ophthalmology, David Geffen School of Medicine at the University of California Los Angeles, Los Angeles, California, United States
[3]Department of Ophthalmology, University of Ottawa, Ottawa, Ontario, Canada
[4]Ottawa Hospital Research Institute, Ottawa, Ontario, Canada

Correspondence: Samuel Asanad, Department of Ophthalmology, David Geffen School of Medicine at the University of California Los Angeles, 10833 Le Conte Ave, Los Angeles, CA 90095, USA; sasanad@mednet.ucla.edu, samuelasanad@gmail.com.

Submitted: December 8, 2018
Accepted: February 22, 2019

Citation: Asanad S, Ross-Cisneros FN, Nassisi M, Barron E, Karanjia R, Sadun AA. The retina in Alzheimer's disease: histomorphometric analysis of an ophthalmologic biomarker. *Invest Ophthalmol Vis Sci*. 2019;60:1491–1500. https://doi.org/10.1167/iovs.18-25966

Purpose. To provide a histopathologic, morphometric analysis of the retina in Alzheimer's disease (AD).

Methods. Human postmortem retinas from eight patients with AD (mean age: 80 ± 12.7 years) and from 11 age-matched controls (mean age: 78 ± 16.57 years) were analyzed. The retinas were sampled from the superior quadrant on both the temporal and nasal sides with respect to the optic nerve. Thickness of the inner and outer layers involving the retinal nerve fiber layer (RNFL), retinal ganglion cell layer (RGCL), inner plexiform layer (IPL), inner nuclear layer (INL), and outer nuclear layer (ONL) were measured and compared between controls and AD. A total of 16 measurements of retinal thickness were acquired for each layer.

Results. RNFL thinning supero-temporally was significant closest to the optic nerve (~35% thickness reduction; $P < 0.001$). Supero-nasally, RNFL was thinner throughout all points (~40% reduction; $P < 0.001$). Supero-temporally, RGCL thinning was pronounced toward the macula (~35% thickness reduction; $P < 0.001$). Supero-nasally, RGCL showed uniform thinning throughout (~35% reduction; $P < 0.001$). IPL thinning supero-temporally was statistically significant in the macula (~15% reduction; $P < 0.01$). Supero-nasal IPL featured uniform thinning throughout (~25% reduction; $P < 0.001$). Supero-temporally, INL and ONL thinning were pronounced toward the macula (~25% reduction; $P < 0.01$). Supero-nasally, INL and ONL were thinner throughout (~25% reduction; $P < 0.01$).

Conclusions. Our study revealed marked thinning in both the inner and outer layers of the retina. These quantified histopathologic findings provide a more comprehensive understanding of the retina in AD than previously reported.

Keywords: Alzheimer's disease, retinal biomarkers, histopathology, morphometric analysis

Alzheimer's disease (AD) is the leading cause of dementia, affecting over 26 million people, and the most expensive disease in America at a total cost of $259 billion in 2017.[1,2] As the field of medicine aims to prolong life, it is not without cost since the number of people suffering from AD, a disease of aging, continues to rise, estimated to quadruple by 2050.[2,3] Therefore, effective and timely diagnostic approaches become critical as therapies are more likely to be effective in earlier stages of the disease rather than later.[4,5]

Aside from cognitive abnormalities, ophthalmologic impairments including visual acuity, color recognition, and motion perception have all been reported in the early stages of dementia even prior to manifesting as a clear diagnosis of AD.[6–12] These symptoms of visual dysfunction in AD have been associated with the degeneration of the optic nerve and retina, developmental outgrowths of the brain,[13–15] since cortical deficits alone do not explain these visual deficits.[11,12,16,17] Ocular manifestations of AD were first shown by our laboratory, whereby the optic nerves of postmortem tissue exhibited diffuse axonal degeneration.[18,19] More recently, hallmark pathologies of neurodegeneration typical for AD in the brain have also been suggested in the retina. We previously demonstrated amyloid β-protein (Aβ) accumulation inside and around melanopsin-immunoreactive RGCs (mRGCs) in AD, possibly explaining circadian rhythm disturbances seen in these patients.[20] Additional studies have identified Aβ plaque pathology in postmortem retinas of definite AD patients as well as in early-stage cases.[1,20–24]

Following the advent of optical coherence tomography (OCT), in vivo studies have revealed significant retinal thinning, suggesting the retina as a potential noninvasive biomarker for the early progressive effects of neurodegeneration in AD.[16,18,25–27] However, the clinical utility of the retina as a purported biomarker for AD remains inconclusive as live patient studies of retinal structure and function in AD have been controversial.[28–33] The majority of these studies have focused on the inner retinal layers including the retinal nerve fiber layer (RNFL) and retinal ganglion cell layer (RGCL) with less attention to the outer retinal layers including the inner nuclear layer (INL) and outer nuclear layer (ONL) thus limiting a comprehensive understanding of the retina in AD. Most AD studies have predominantly assessed the retina with OCT,

Table 1. Demographic Data for Control Tissue Samples

ID	Age at Death	Sex	Race	Postmortem Interval, h	Cause of Death
C1	54	M	Caucasian	6.0	Anoxic brain injury secondary to acute myocardial infarction
C2	60	M	Caucasian	7.3	Metastatic lung cancer
C3	64	F	Caucasian	11.0	Cardiogenic shock secondary to congestive heart failure
C4	70	F	Caucasian	10.8	End-stage chronic obstructive pulmonary disease
C5	74	M	Caucasian	7.2	Ruptured brain aneurysm
C6	80	M	Caucasian	18.5	Respiratory failure secondary to postoperative sequelae
C7	80	M	Caucasian	13.2	Sudden respiratory failure secondary to pneumonia
C8	85	M	Caucasian	11.5	Gastrointestinal bleeding
C9	93	M	Caucasian	6.5	Subarachnoid hemorrhage
C10	95	F	Caucasian	3.3	N.A.
C11	105	F	Caucasian	6.0	Cardiopulmonary arrest

C, control; F, female; M, male; N.A., not available.

which has various limitations. These include reduced cooperation in cognitively compromised patients, especially in advanced stages, and the persistent challenge of unequivocally diagnosing AD clinically. Further deviations in reported results may arise from intrinsic apparatus variability including optic disc centering procedures, eye tracking system, length of examination time, and anatomical errors frequently associated with OCT interpretation.[28,34,35] Given these inconsistencies with using an in vivo approach to evaluate the retina in AD, we pursued an ex vivo approach using human postmortem tissue to allow for a more precise, quantitative assessment of the retina as a potential ophthalmologic biomarker for AD.

Methods

Human Tissues

Human postmortem control eyes were received from the Lions VisionGift eye bank in Portland, Oregon, and the AD eyes were acquired through the Alzheimer's Disease Research Center (ADRC) Neuropathology Core at the University of Southern California (USC), funded by the National Institute of Aging. The Institutional Review Board (IRB) at USC approved the acquisition of donor tissue through the ADRC at USC. All experiments were performed in accordance with the relevant guidelines and regulations as detailed by the IRB at USC. The need to obtain informed consent was waived by the IRB since the tissues were de-identified prior to distribution. We analyzed one eye from each postmortem subject, which included eight patients with AD (mean age, 80 ± 12.7 years) (Table 1) and 11 age-matched control subjects (mean age, 78 ± 16.6 years) derived at autopsy (Table 2). The groups did not differ significantly in age or years of education.

Cognitive Evaluation and AD Diagnosis

The diagnosis of AD was confirmed neuropathologically in accordance with modified Consortium to Establish a Registry for Alzheimer's Disease (CERAD) or National Institute on Aging (NIA)-Reagan criteria and Braak–Braak Alzheimer classification.[36] Clinical charts of controls and AD patients were reviewed. Age-matched eyes from patients without an AD diagnosis served as control specimens in the study. The inclusion criteria for AD cases included a neuropathological diagnosis of high likelihood AD according to NIA–Reagan Institute criteria,[37] frequent neuritic plaques according to modified CERAD criteria,[36] and Braak stage V or VI,[38] based on the neuropathological reports (C. Miller, MD, ADRC at USC). Exclusion criteria were co-occurring and/or confounding ophthalmologic diseases. Tissues with significant posterior pole ocular pathology such as age-related macular degeneration, optic neuropathies such as glaucoma, ischemic optic neuropathy, and diabetic retinopathy were not included in the study. Moreover, exclusion criteria for controls provided by the eye tissue banks were the presence of neurological and psychiatric disorders, treatment with chemotherapeutic agents prior to death, human immunodeficiency virus infection, alcohol abuse, and diabetes.

Histology

Postmortem tissue samples used in the current study were previously immunohistochemically evaluated for retinal Aβ using an established protocol.[20] The AD group demonstrated positive immunoreactivity for substantial retinal Aβ deposition. Control tissues demonstrated minimal to no immunoreactivity for retinal Aβ deposition. Eyes were immersion-fixed in 10% neutral buffered formalin. Eyes were dissected horizontally through the upper region of the optic nerve extending circumferentially through the superior nasal and temporal retinas. This single ribbon of tissue was processed and embedded into paraffin blocks, sectioned at 5 μm on a retracting microtome, and stained with hematoxylin and eosin. A published, detailed description of this tissue preparation and staining protocol is available for reference.[20]

Morphometric Analysis

Digitized histopathology images of the control and AD retinas were acquired using the Aperio Scanscope-model CS2 (Leica Biosystems, Buffalo Grove, IL, USA) equipped with a five-slide capacity and high-resolution magnification capabilities using a line scanning method. The 40× lens on the digital pathology scanner produced a rapid and seamless image of the retina including the entire nasal and temporal regions in a single section. The system was calibrated before each measurement session at 0.25 μM/pixel linked with the 40× scanning lens protocol.[39]

As illustrated in Figure 1, postmortem histology permitted a more precise and feasible evaluation of the retinal layers in comparison with OCT. Thickness measurements were manually performed for the inner retinal layers including the RNFL, RGCL, and inner plexiform layer (IPL), which together comprise the retinal ganglion cell complex (RGCC). We also measured the thicknesses of the nuclear layers comprising the outer retina, specifically the INL and ONL. As seen in Figure 1B, RNFL thickness was defined as the distance from the outer aspect of the inner limiting membrane to the inner border of the RGCL. RGCL thickness was defined as the distance from the outer aspect of the RNFL to the inner border of the IPL. IPL thickness was defined as the distance from the outer RGCL to the inner border of the INL. INL thickness was defined as the

Table 2. Demographic Data for AD Tissue Samples

ID	Age at Death	Sex	Race	Postmortem Interval, h	Disease Duration	BRAAK Stage
A1	51	F	Caucasian	6.0	N.A.	VI
A2	62	M	Caucasian	5.8	4	V
A3	75	F	Caucasian	5.5	7	V
A4	81	M	Caucasian	4.0	11	VI
A5	86	M	Caucasian	6.0	6	VI
A6	95	F	Caucasian	6.0	11	V
A7	96	F	Hispanic	6.0	10	V
A8	98	F	Caucasian	7.5	N.A.	V

Cause of death was not known due to inaccessibility of death certificates through the USC ADRC from which the postmortem tissues were acquired. A, Alzheimer's disease; F, female; M, male; N.A., not available.

distance from the outer IPL to the inner border of the outer plexiform layer (OPL). ONL thickness was defined as the distance from the outer OPL to the inner border of the photoreceptor layer. Thickness measurements were performed using ImageScope v12.1.0.5029 software (Leica Biosystems) and were obtained at approximately every 500 μm spanning the total distance beginning from the middle of the optic nerve to the center of the macula within the superior ribbon of tissue. This amounted to a total of eight measuring points for each layer supero-temporally (Fig. 2). Additionally, the same total distance was projected supero-nasally relative to the optic nerve with thickness measurements performed again at approximately every 500 μm for a total of eight measuring points for each layer supero-nasally (Fig. 2). The validities of the performed measurements were subsequently assessed by a masked histopathologist.

Statistical Methods

Statistical analysis was performed using SPSS V.20 package software. To compare the groups, independent *t*-test and Mann-Whitney *U* test were applied. The normality assumption for the independent variables was checked with Shapiro-Wilk test. The variables that were compliant with the normality assumption were subjected to independent *t*-test, while those that did not meet the normality assumption were subjected to Mann-Whitney *U* test. Statistical significance was established at $P < 0.05$.

Results

Qualitative Findings

The RNFL was remarkably thinner in AD relative to controls as seen on light microscopy in Figure 3. The RGCL in AD was also markedly thinner and showed an appreciable dropout of nuclei relative to controls (Fig. 4) on qualitative assessment. IPL thinning was not grossly remarkable in AD. However, the density of plexiform fibers on visual inspection was appreciably less in AD relative to controls (Fig. 5). The INL and ONL in AD were markedly thinner and showed an appreciable dropout of nuclei relative to controls (Fig. 4).

Retinal Nerve Fiber Layer

Quantitatively (Fig. 6), RNFL thinning supero-temporally was most pronounced in the peripapillary region, closest to the optic nerve. Supero-nasally, the RNFL was markedly thinner throughout all measured regions, most pronounced in the peripapillary region. Overall, the RNFL was significantly thinner supero-nasally than supero-temporally.

Retinal Ganglion Cell Layer

Quantitative analysis (Fig. 7) of the supero-temporal region revealed RGCL thinning most pronounced toward the macula. The supero-nasal region showed uniform thinning across all measured areas.

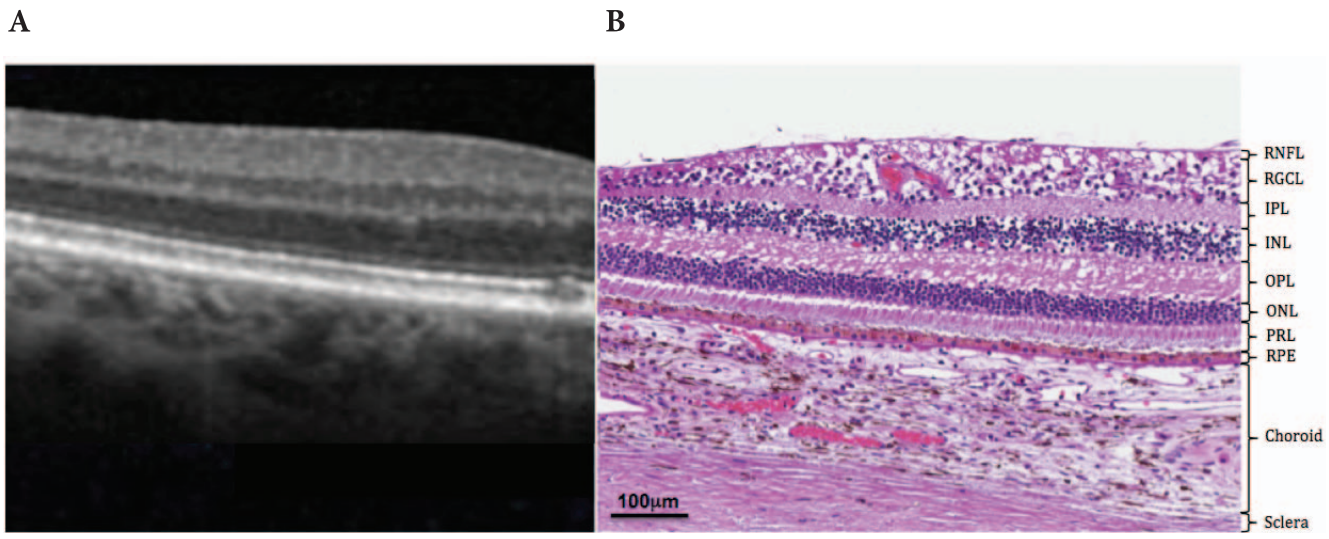

Figure 1. Illustrates challenges of retinal layer identification on enhanced depth imaging optical coherence tomography (EDI-OCT) (**A**) relative to accurate identification and delineation of the corresponding retinal layers on histology in a representative control micrograph stained with hematoxylin and eosin (**B**) within the macula.

Investigative Ophthalmology & Visual Science

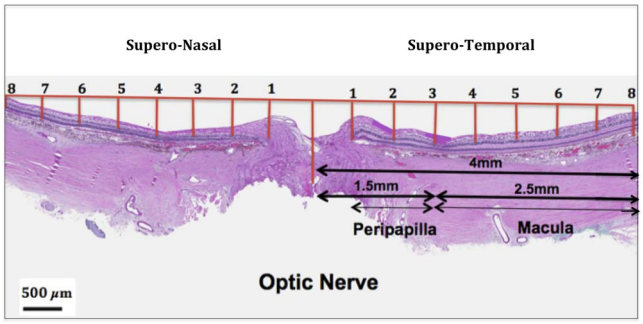

Figure 2. Morphometric analysis of the retinal layers. Thickness measurements were acquired along eight points beginning from the middle of the optic nerve to the macular region supero-temporally. The same distance was applied to the supero-nasal side, resulting in a total of 16 total thickness measurements for all five retinal layers.

Inner Plexiform Layer

On quantitative assessment (Fig. 8), IPL thinning supero-temporally was statistically significant solely in the macula, but otherwise unremarkable relative to controls. In contrast, the supero-nasal IPL featured substantial, uniform thinning throughout. Overall, the IPL was considerably thinner supero-nasally than supero-temporally.

Inner Nuclear Layer

As seen in Figure 9, quantitative analysis showed significant supero-temporal thinning most pronounced toward the macula. Supero-nasally, the INL was significantly thinner throughout although most pronounced toward the optic nerve and with decreasing severity out to the peripheral retina.

Outer Nuclear Layer

As seen in Figure 10, quantitative analysis showed significant supero-temporal thinning of the ONL most pronounced toward the macula. Supero-nasally, the ONL was significantly thinner in the regions closest to the optic nerve and with decreasing severity out to the peripheral retina.

Discussion

The present study performed a morphometric analysis of the retina in AD. We provide, for the first time, a quantitative thickness assessment of the inner (RNFL, RGCL, IPL) and outer layers (INL and ONL) of the retina using postmortem human tissues. These tissues were histopathologically confirmed for amyloid deposition and were derived from patients neuropathologically confirmed for severe AD. We found significant thinning for all assessed retinal layers and observed differences in thickness by layer and by region, supero-nasally and supero-temporally with respect to the optic nerve. Taken together,

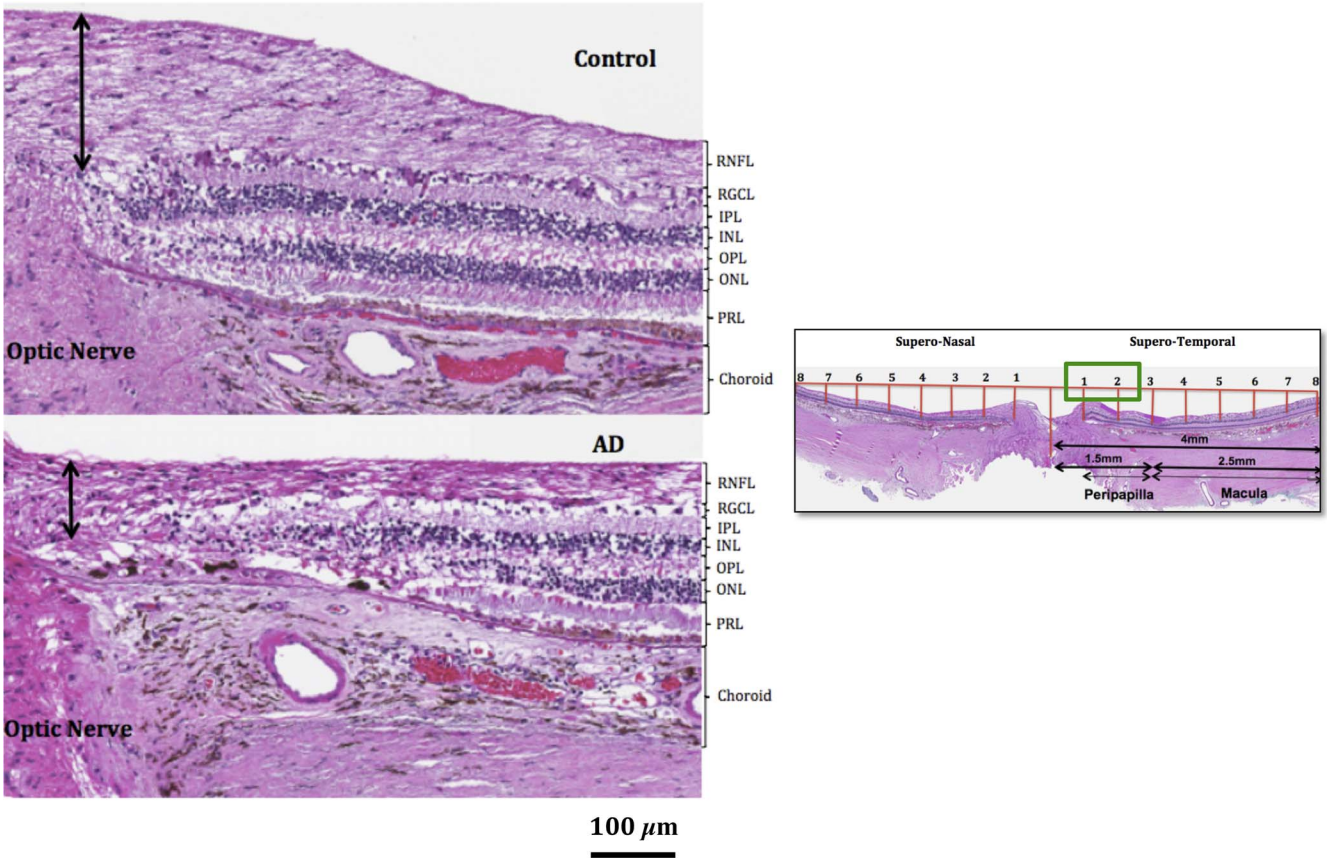

Figure 3. Supero-temporal RNFL thickness (*black arrows*) in control (*top*) and AD postmortem tissue (*bottom*) on light microscopy. Depicts supero-temporal RNFL thinning most pronounced closest to the optic nerve. Low magnification view of the retina is depicted on the right with the corresponding retinal region marked (*green box*).

Investigative Ophthalmology & Visual Science

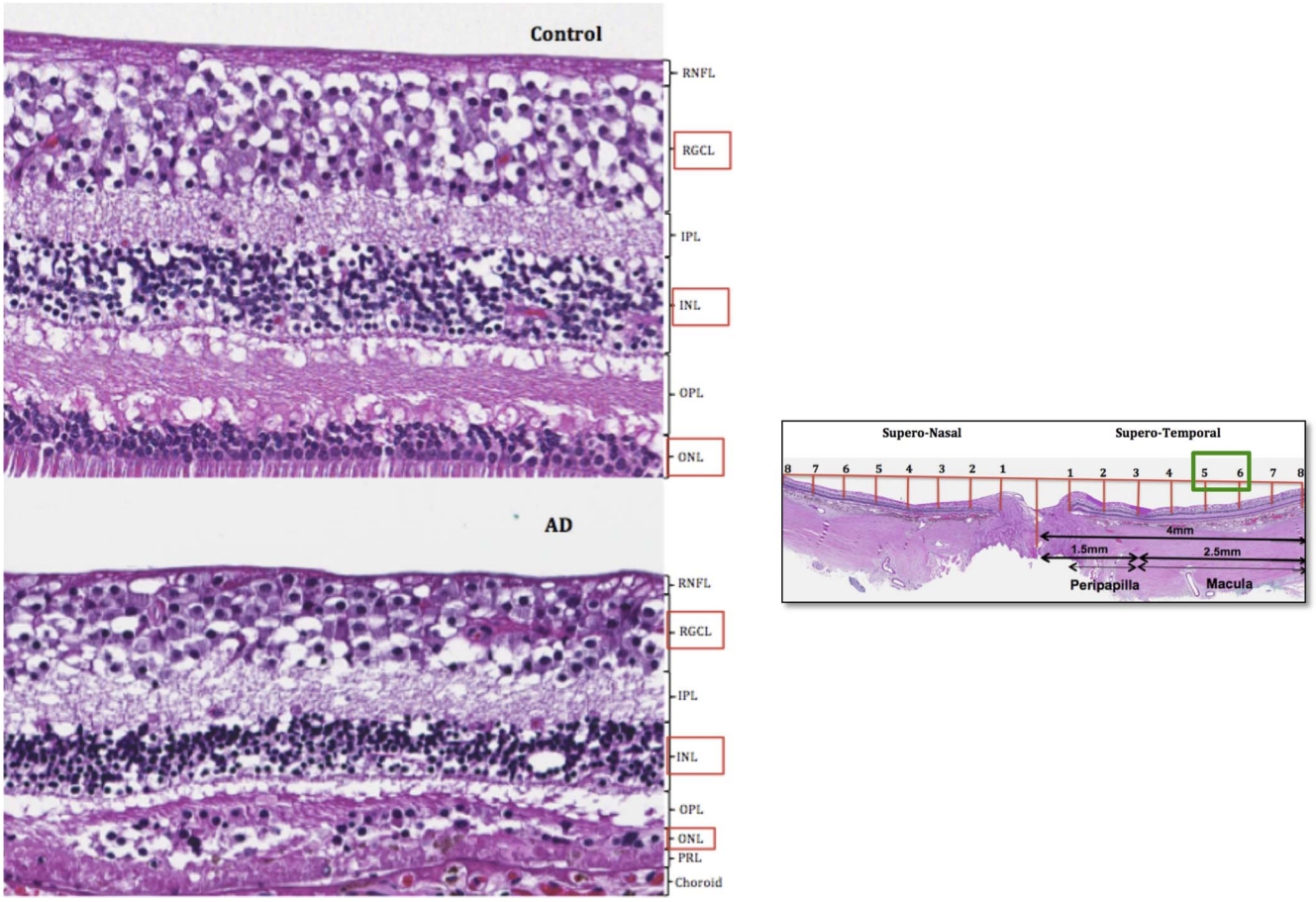

Figure 4. Qualitative assessment of the supero-temporal RGCL, INL, and ONL (marked by *red boxes*) in representative control (*top*) and AD (*bottom*) micrographs on light microscopy. Depicts supero-temporal RGCL, INL, and ONL thinning most pronounced in the macular region. Low magnification view of the retina is depicted on the right with the corresponding retinal region marked (*green box*).

these findings expand our understanding of the retina as a potential surrogate biomarker for AD and propose an objective, quantifiable means of assessing this disease.

Histological examination of the RNFL revealed significant thinning closest to the optic nerve in the superior-temporal region. In the superior-nasal region, we found diffuse thinning throughout the RNFL, most pronounced closest to the optic nerve. This thickness profile matches the distribution of the retinal Aβ deposits in the mid- and far-periphery of the superior quadrants of these tissues as previously demonstrated by our laboratory.[20,40,41] Similarly, Koronyo and colleagues[23,42] described an extensive loss of neurons in the superior quadrant and the mid- and far-peripheries. Interestingly, the supero-nasal RNFL was markedly thinner overall compared to the supero-temporal RNFL. This is consistent with our previous findings where axonal loss predominantly affected the larger fibers and spared the smaller fibers, similarly observed by Koronyo and colleagues.[20,23,42]

Our study also histologically assessed RGCL and IPL thickness. While thickness changes for these layers have been previously reported in vivo using OCT, these studies predominantly evaluated the RGCL and IPL as a combined thickness and exclusively in the macula.[28–33] Since AD in the eye has been characterized as a disease primarily of the ganglion cells, we expand upon these studies by assessing the RGCL and IPL separately rather than combined, and geographically beyond the macula. Supero-temporally to the optic nerve, RGCL thinning was most severe toward the macula. However, supero-nasally, RGCL thinning extended uniformly out to the peripheral retina. Similarly, significant thinning of the supero-temporal IPL was seen in the macula with uniform thinning out to the periphery supero-nasally. This IPL atrophy may likely contribute to deficiencies in motion perception and contrast sensitivity frequently seen in patients with AD since processing of these visual stimuli begins in this layer.[43,44] Intriguingly, the IPL exhibited roughly half the magnitude of thickness reduction in comparison with the RNFL and RGCL. This is in parallel with the distribution of Aβ seen in these tissues, whereby Aβ deposits were found to be more concentrated in the RGCL relative to the IPL.[20] This finding also suggests that atrophy of the IPL, comprised of ganglion cell synaptic connections, dendrites, and bipolar cells, may likely be secondarily involved and follow after ganglion cell and nerve fiber loss. Previous studies have suggested IPL changes may precede RGCL changes. Williams et al.[45] found IPL loss prior to RGCL loss in a mouse model, while Snyder et al.[46] showed IPL thickening correlating with amyloid deposition in preclinical AD patients. However, animal models are not always truly representative of human disease,[45] and the limitations of OCT studies may persist without histopathologically confirming fibrillar Aβ within the inclusion bodies seen on live imaging.[47] The present study was performed in postmortem human eyes in severe stages of AD.

Thickness assessment of the outer retina showed remarkable thinning of both the INL and ONL. Supero-temporally to the optic nerve, INL thinning was significantly apparent throughout all measured points and most severe toward the

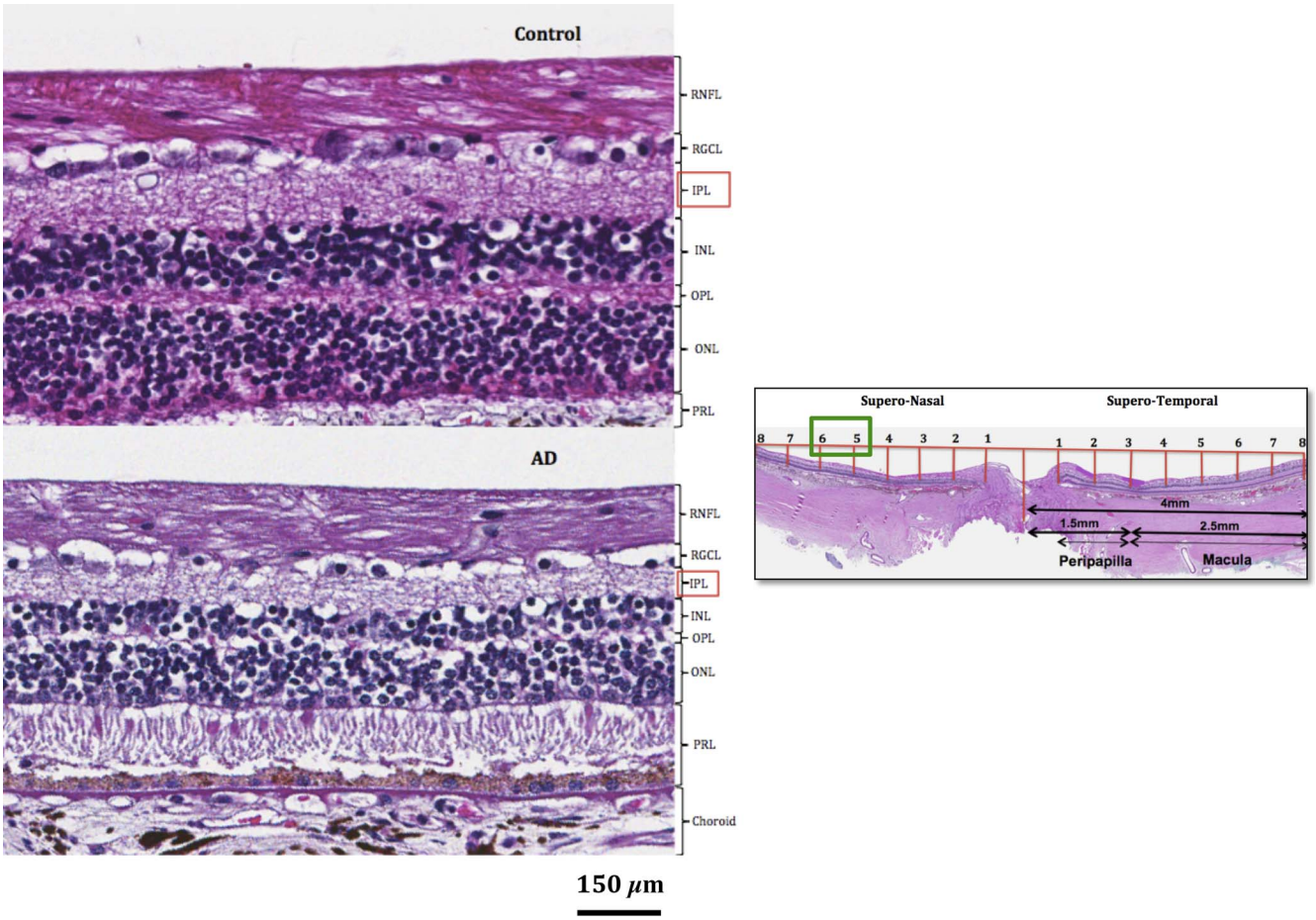

Figure 5. Qualitative assessment of the IPL (marked by *red box*) in representative control (*top*) and AD (*bottom*) micrographs on light microscopy. Depicts IPL thinning most pronounced supero-nasally relative to the optic nerve. Low magnification view of the retina is depicted on the right with the corresponding retinal region marked (*green box*).

macula. Supero-nasally, INL thinning was also significantly thinner across all measured points and most severe toward the optic nerve. Similar to the INL, significant ONL thinning was observed throughout all measured points and most severe toward the macula supero-temporally relative to the optic nerve. Also resembling the INL, ONL thinning supero-nasally was significantly thinner across all measured points and most severe toward the optic nerve. Therefore, the INL and ONL shared similar thickness profiles in AD. Intriguingly, the magnitude of thickness reduction for the INL and ONL was notably less than that of the RNFL and RGCL. These thickness findings may be explained by the distribution of the retinal Aβ deposits, which were more concentrated in the RGCL and to a lesser extent in the INL and ONL.[20] Similarly, Koronyo-Hamaoui et al.[23] observed neuronal reduction in the INL and ONL accompanied by retinal Aβ pathology.

The observed pattern of retinal thinning in AD, whereby thinning was greatest for the inner layers of the retina followed by the outer layers, may likely be attributed to Aβ deposition and consequent neurotoxicity as suggested by previous studies.[20,23,42,47,48] Notably, however, the IPL was less severely thinned relative to the INL and ONL. The INL consists of the cell bodies of horizontal cells, bipolar cells, and amacrine cells, while the ONL consists of photoreceptor cell bodies.[43] In the context of severe AD, tissue loss in these layers may be associated with retrograde transsynaptic degeneration.[49] However, future studies assessing the morphological changes of the various cell types comprising these retinal layers would be necessary to support this hypothesis.

While our measurements may have been impacted by postmortem tissue swelling and tissue shrinkage as induced by fixation, both tissue groups were prepared under identical protocols and deviations would be equally distributed between both AD and controls, mitigating measurement bias. Despite its limited sample size, the current study represents the largest histological analysis of retinal thickness in AD. Including only one eye for each patient is a particular strength of our study as it avoids artificial sample size enhancement, which may have arisen from including both eyes. In addition, we used 16 measurements per layer to account for case-specific differences in retinal structure, further strengthening the significance of our findings. We did not assess the OPL and photoreceptor layer as these layers exhibited fragmentation artifacts following tissue preparation. Glaucoma is another common ocular disease that has been implicated as sharing commonalities with AD.[21] However, the relationship between these two disease entities remains controversial and additional studies are warranted to investigate their similarities.

Conclusions and Future Directions

We provide the first, morphometric analysis of both the inner and outer retinal layers using postmortem tissue histologically confirmed for Aβ derived from patients neuropathologically

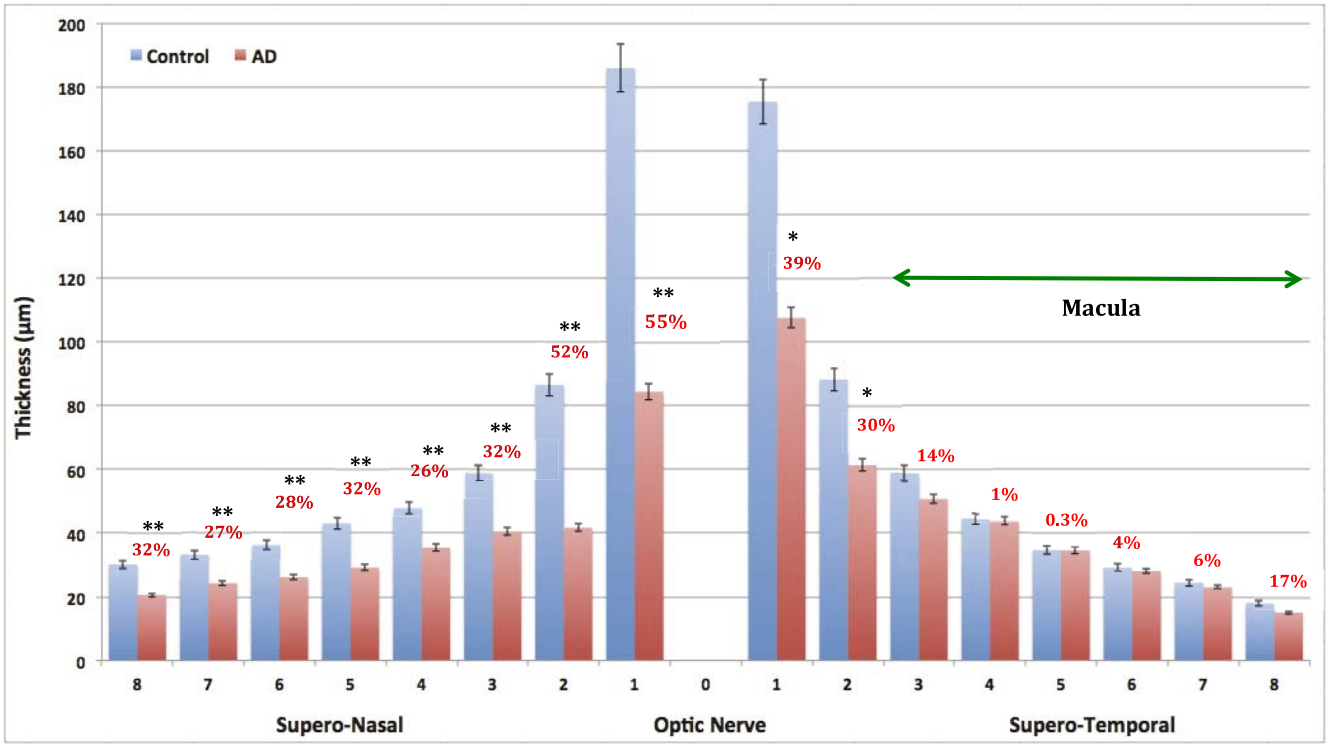

Figure 6. Average RNFL thickness comparison per sector between controls (*blue*) and AD (*red*) tissue samples (*$P < 0.05$; **$P < 0.001$). Error bars denote standard deviation.

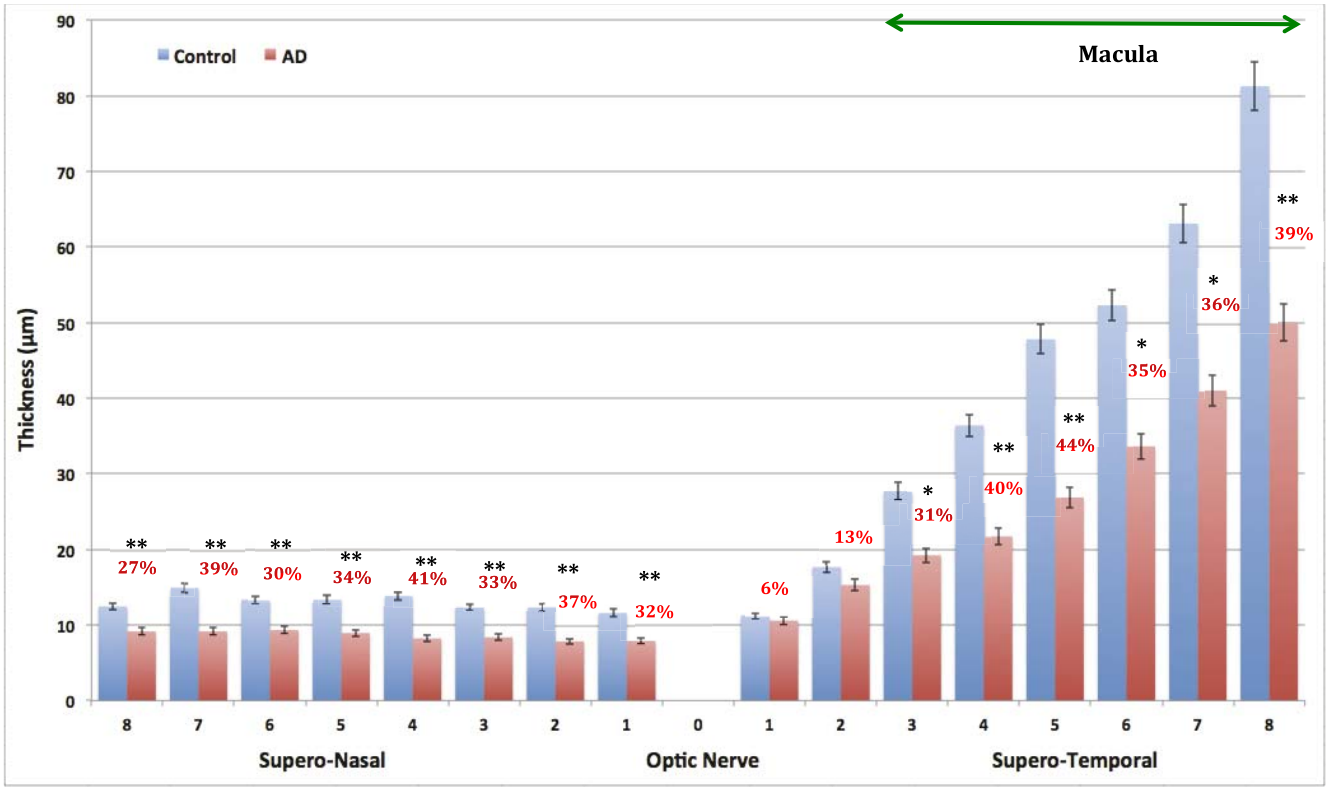

Figure 7. Average RGCL thickness comparison per sector between controls (*blue*) and AD (*red*) tissue samples (*$P < 0.05$; **$P < 0.001$). Error bars denote standard deviation.

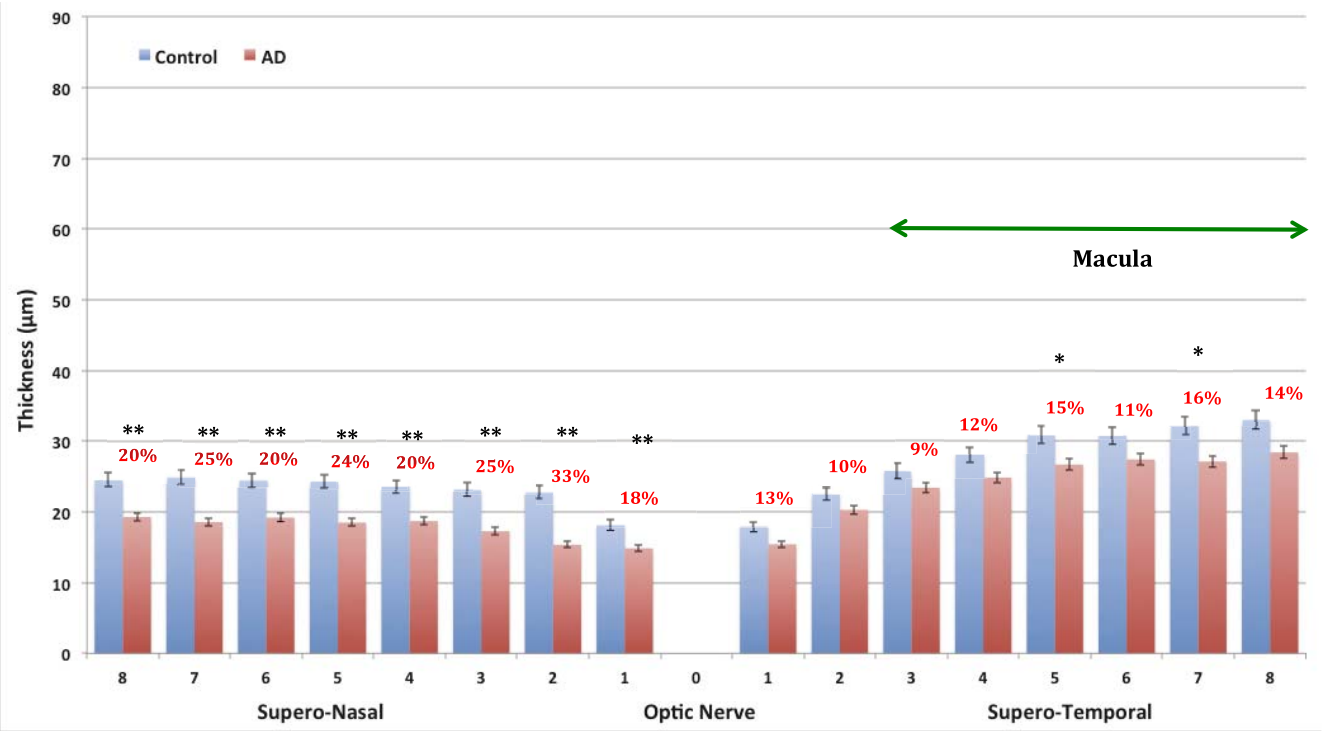

FIGURE 8. Average IPL thickness comparison per sector between controls (*blue*) and AD (*red*) tissue samples (*$P < 0.05$; **$P < 0.01$). Error bars denote standard deviation.

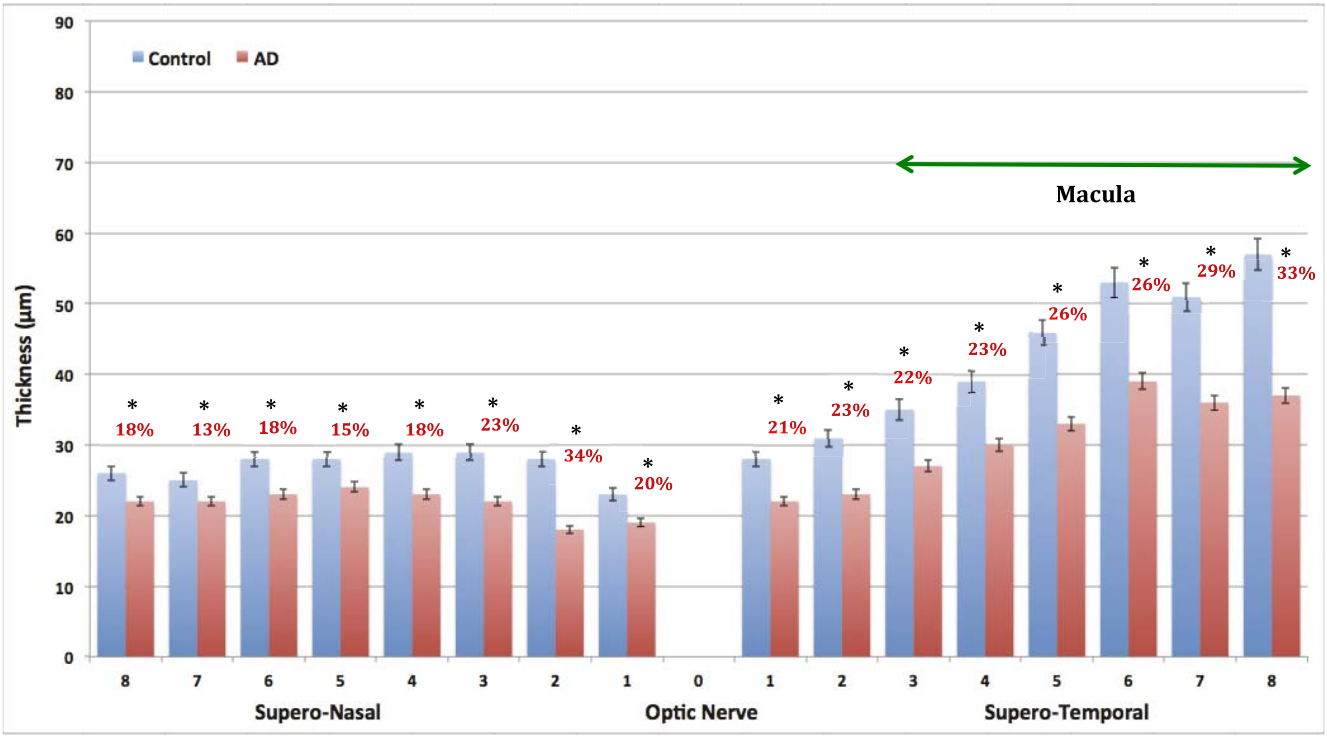

FIGURE 9. Average INL thickness comparison per sector between controls (*blue*) and AD (*red*) tissue samples (*$P < 0.05$). Error bars denote standard deviation.

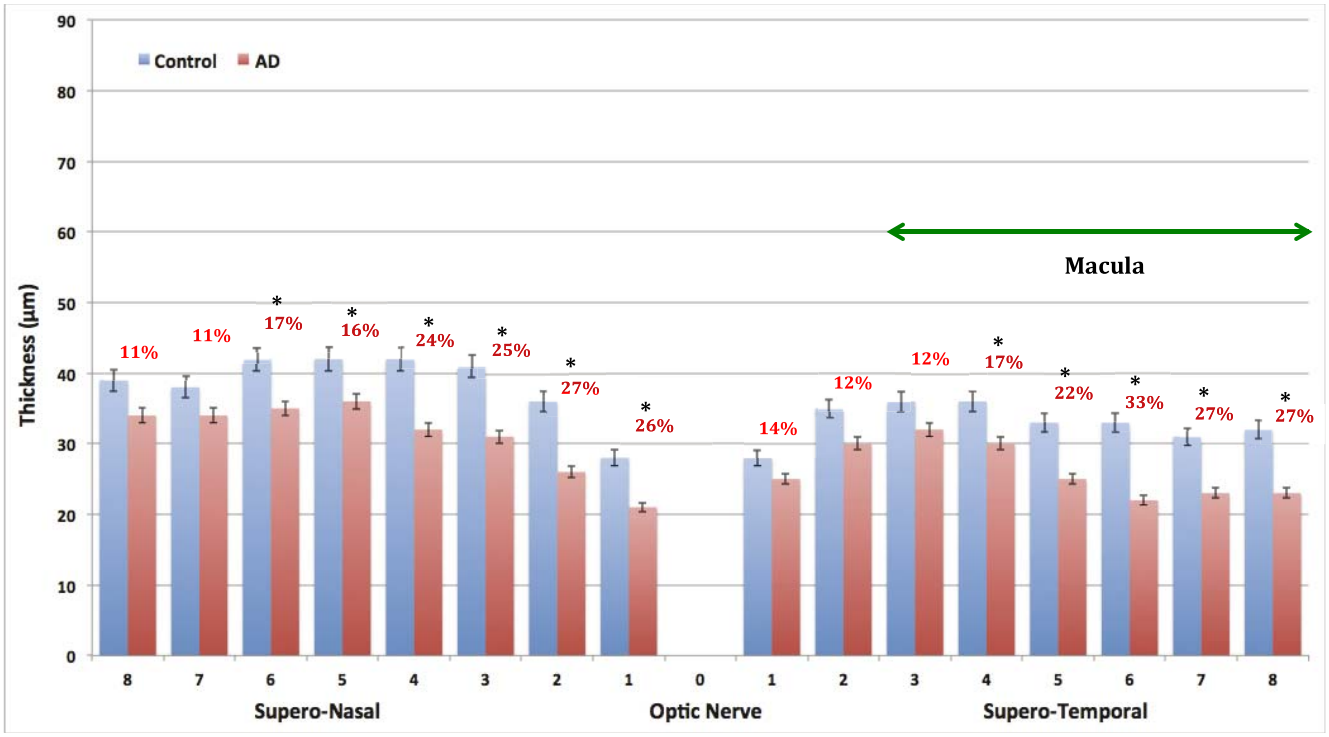

Figure 10. Average ONL thickness comparison per sector between controls (*blue*) and AD (*red*) tissue samples (*$P < 0.05$). Error bars denote standard deviation.

confirmed for severe AD. Different patterns of thinning were exhibited in the superior-nasal and superior-temporal regions of the retina relative to the optic nerve. We also found a gradient of thickness reduction whereby thinning was greatest for the inner layers of the retina followed by the outer layers of the retina. A more comprehensive understanding of the retina as measured ex vivo can be useful for assessing the clinical validity and utility of the retina, a purported ocular biomarker in vivo using OCT. Given mounting evidence that alterations in the visual system may precede cognitive changes, such a quantitative means of assessing disease may serve useful for ultimately monitoring disease, which may permit earlier interventions. Therefore, future studies are suggested. Our laboratory had originally demonstrated optic nerve degeneration in AD on histopathology. Following the advent of OCT, studies have primarily assessed retinal thickness changes in the macula to explain the visual symptoms experienced by AD patients. Given these findings, the current morphometric analysis specifically focused on near and mid peripheral retina to evaluate thickness changes in relation to distance from the optic nerve and the central-superior region of the macula. Notably, recent studies have also identified significant amyloid deposition in the far peripheral retina. Additional studies assessing associated retinal thickness changes in these regions may be warranted and serve beneficial. Furthermore, our study focused on AD tissues derived from patients with severe AD (BRAAK stages V and VI). Histological comparisons from earlier disease stages would be worthwhile to assess thickness changes as a function of disease severity.

Acknowledgments

The authors thank the Lions VisionGift eye bank and the Alzheimer's Disease Research Center (ADRC) Neuropathology Core at the University of Southern California (USC) for providing the tissue samples for this study. We also thank our funding sources including Research to Prevent Blindness, Inc. (RPB), the National Institute of Aging (NIA), and the International Foundation for Optic Nerve Diseases (IFOND).

Supported by NIH National Institute on Aging Grant #P50-AG05142 (USC ADRC Neuropathology Core Grant), Research to Prevent Blindness, Inc. (unrestricted grant), and the International Foundation for Optic Nerve Diseases (IFOND).

Disclosure: **S. Asanad,** Research to Prevent Blindness, Inc. (F); **F.N. Ross-Cisneros**, None; **M. Nassisi**, None; **E. Barron**, None; **R. Karanjia**, None; **A.A. Sadun**, Research to Prevent Blindness, Inc. (F)

References

1. Tsai Y, Lu B, Ljubimov AV, et al. Ocular changes in TgF344-AD rat model of Alzheimer's disease. *Invest Ophthalmol Vis Sci*. 2014;55:523–534.
2. Batsch NL, Mittelman MS, eds. *World Alzheimer Report 2012: Overcoming the Stigma of Dementia*. London: Alzheimer's Disease International; 2012:75.
3. Holtzman DM, Morris JC, Goate AM. Alzheimer's disease: the challenge of the second century. *Sci Transl Med*. 2011;3:77sr1.
4. Uhlmann RF, Larson EB, Koepsell TD, Rees TS, Duckert LG. Visual impairment and cognitive dysfunction in Alzheimer's disease. *J Gen Intern Med*. 1991;6:126–132.
5. Guo L, Salt TE, Maass A, et al. Assessment of neuroprotective effects of glutamate modulation on glaucoma-related retinal ganglion cell apoptosis in vivo. *Invest Ophthalmol Vis Sci*. 2006;47:626–633.
6. Javaid FZ, Brenton J, Guo L, Cordeiro MF. Visual and ocular manifestations of AD and their use as biomarkers for diagnosis and progression. *Front Neurol*. 2016;7:55.
7. Sadun AA. Axon caliber populations in the human optic nerve: change with age and disease. *Int Neuro-Oph Society*. 1986:5–20.
8. Zanetti O, Solerte SB, Cantoni F. Life expectancy in Alzheimer's disease. *Arch Gerontol Geriatr*. 2009;(49 suppl 1):237–243.

9. Katz B, Rimmer S. Ophthalmologic manifestations of Alzheimer's disease. *Surv Ophthalmol*. 1989;34:31–43.
10. Salamone G, Di lorenzo C, Mosti S, et al. Color discrimination performance in patients with Alzheimer's disease. *Dement Geriatr Cogn Disord*. 2009;27:501–507.
11. Tzekov R, Mullan M. Vision function abnormalities in Alzheimer disease. *Surv Ophthalmol*. 2014;59:414–433.
12. Dugger BN, Tu M, Murray ME, Dickson DW. Disease specificity and pathologic progression of tau pathology in brainstem nuclei of Alzheimer's disease and progressive supranuclear palsy. *Neurosci Lett*. 2011;491:122–126.
13. Purves D, Augsutine GJ, Fitzpatrick D, et al. Vision: the eye: the retina. In: *Neuroscience*. 2nd ed. Sunderland, MA: Sinauer Associates; 2001: chap 11.
14. Byerly MS, Blackshaw S. Vertebrate retina and hypothalamus development. *Wiley Interdiscip Rev Syst Biol Med*. 2009;1:380–389.
15. Trost A, Lange S, Schroedl F, et al. Brain and retinal pericytes: origin, function and role. *Front Cell Neurosci*. 2016;10:20.
16. Thomson K, Yeo JM, Waddell B, Cameron JR, Pai S. A systematic review and meta- analysis of RNFL change in dementia, using OCT. *Alzheimers Dement (Amst)*. 2015;1:136–143.
17. Sadun A, Borchert M, DeVita E, et al. Assessment of visual impairment in patients with Alzheimer's disease. *Am J Ophthalmol*. 1987;104:113–120.
18. Liu D, Zhang L, Li Z, et al. Thinner changes of the retinal nerve fiber layer in patients with mild cognitive impairment and Alzheimer's disease. *BMC Neurol*. 2015;15:14.
19. Hinton DR, Sadun AA, Blanks JC, Miller CA. Optic-nerve degeneration in Alzheimer's disease. *N Engl J Med*. 1986;315:485–487.
20. La Morgia C, Ross-Cisneros FN, Koronyo Y, et al. Melanopsin retinal ganglion cell loss in Alzheimer disease. *Ann Neurol*. 2016;79:90–109.
21. Hart NJ, Koronyo Y, Black KL, Koronyo-Hamaoui M. Ocular indicators of Alzheimer's: exploring disease in the retina. *Acta Neuropathol*. 2016;132:767–787.
22. Alexandrov PN, Pogue A, Bhattacharjee S, Lukiw WJ. Retinal amyloid peptides and complement factor H in transgenic models of Alzheimer's disease. *Neuroreport*. 2011;22:623–627.
23. Koronyo-Hamaoui M, Koronyo Y, Ljubimov AV, et al. Identification of amyloid plaques in retinas from Alzheimer's patients and noninvasive in vivo optical imaging of retinal plaques in a mouse model. *Neuroimage*. 2011;54(suppl 1):S204–S217.
24. Schön C, Hoffmann NA, Ochs SM, et al. Long-term in vivo imaging of fibrillar tau in the retina of P301S transgenic mice. *PLoS One*. 2012;7:e53547.
25. Garcia-Martin E, Rodriguez-Mena D, Herrero R, et al. Neuro-ophthalmologic evaluation, quality of life, and functional disability in patients with MS. *Neurology*. 2013;81:76–83.
26. Garcia-Martin E, Bambo MP, Marques ML, et al. Ganglion cell layer measurements correlate with disease severity in patients with Alzheimer's disease. *Acta Ophthalmologica*. 2016;94:454–459.
27. Chan VTT, Sun Z, Tang S, et al. Spectral domain-optical coherence tomography measurements in Alzheimer's disease: a systematic review and meta-analysis [published online ahead of print August 13, 2018]. *Ophthalmology*. doi:10.1016/j.ophtha.2018.08.009.
28. Coppola G, Renzo AD, Ziccardi L, et al. Optical coherence tomography in Alzheimer's disease: a meta-analysis. *PLoS One*. 2015;10:e0134750.
29. Shen Y, Shi Z, Jia R, et al. The attenuation of retinal nerve fiber layer thickness and cognitive deterioration. *Front Cell Neurosci*. 2013;7:142.
30. Shen Y, Liu L, Cheng Y, et al. Retinal nerve fiber layer thickness is associated with episodic memory deficit in mild cognitive impairment patients. *Curr Alzheimer Res*. 2014;11:259–266.
31. Shi Z, Wu Y, Wang M, et al. Greater attenuation of retinal nerve fiber layer thickness in Alzheimer's disease patients. *J Alzheimers Dis*. 2014;40:277–283.
32. Kromer R, Serbecic N, Hausner L, Froelich L, Aboul-Enein F, Beutelspacher SC. Detection of retinal nerve fiber layer defects in Alzheimer's disease using SD-OCT. *Front Psychiatry*. 2014;5:22.
33. Ascaso F, Cruz N, Modrego P, et al. Retinal alterations in mild cognitive impairment and Alzheimer's disease: an optical coherence tomography study. *J Neurol*. 2014;261:1522–1530.
34. Spaide R, Curcio CA. Anatomic correlates to the bands seen in the outer retina by optical coherence tomography: literature review and model. *Retina*. 2011;31:1609–1619.
35. Staurenghi G, Sadda S, Chakravarthy U, Spaide RF. Proposed lexicon for anatomic landmarks in normal posterior segment spectral-domain optical coherence tomography: the IN*OCT Consensus. *Ophthalmology*. 2014;121:1572–1578.
36. Mirra SS, Heyman A, McKeel D, et al. The Consortium to Establish a Registry for Alzheimer's Disease (CERAD). Part II. Standardization of the neuropathologic assessment of Alzheimer's disease. *Neurology*. 1991;41:479–486.
37. Hyman BT, Trojanowski JQ. Consensus recommendations for the postmortem diagnosis of Alzheimer disease from the National Institute on Aging and the Reagan Institute Working Group on diagnostic criteria for the neuropathological assessment of Alzheimer disease. *J Neuropathol Exp Neurol*. 1997;56:1095–1097.
38. Braak H, Braak E. Staging of Alzheimer's disease-related neurofibrillary changes. *Neurobiol Aging*. 1995;16:271–278.
39. Webster JD, Dunstan RW. Whole-slide imaging and automated image analysis: considerations and opportunities in the practice of pathology. *Vet Pathol*. 2014;51:211–223.
40. Blanks JC, Hinton DR, Sadun AA. Retinal ganglion cell degeneration in Alzheimer's disease. *Brain Res*. 1989;501:364–372.
41. Blanks JC, Torigoe Y, Hinton DR, et al. Retinal pathology in Alzheimer's disease. I. Ganglion cell loss in foveal/parafoveal retina. *Neurobiol Aging*. 1996;17:377–384.
42. Koronyo Y, Biggs D, Barron E, et al. Retinal amyloid pathology and proof-of-concept imaging trial in Alzheimer's disease. *JCI Insight*. 2017;2:93621.
43. Sadun AA, Borchert M, DeVita E, et al. Assessment of visual impairment in patients with Alzheimer's disease. *Am J Ophthalmol*. 1987;104:113–120.
44. Remington LAR. *Clinical Anatomy and Physiology of the Visual System*. 3rd ed. Oxford, UK: Butter Worth Heinemann; 2012:61–92.
45. Williams PA, Thirgood RA, Oliphant H, et al. Retinal ganglion cell dendritic degeneration in a mouse model of Alzheimer's disease. *Neurobiol Aging*. 2013;34:1799–1806.
46. Snyder PJ, Johnson LN, Lim YY, et al. Nonvascular retinal imaging markers of preclinical Alzheimer's disease. *Alzheimers Dement (Amst)*. 2016;4:169–178.
47. Choi SH, Park SJ, Kim NR. Macular ganglion cell-inner plexiform layer thickness is associated with clinical progression in mild cognitive impairment and Alzheimers disease. *PLoS One*. 2016;11:e0162202.
48. Cunha JP, Moura-Coelho N, Proenca RP, et al. Alzheimer's disease: a review of its visual system neuropathology. Optical coherence tomography—a potential role as a study tool in vivo. *Graefes Arch Clin Exp Ophthalmol*. 2016;254:2079–2092.
49. Santos CY, Johnson LN, Sinoff SE, Festa EK, Heindel WC, Snyder PJ. Change in retinal structural anatomy during the preclinical stage of Alzheimer's disease. *Alzheimers Dement (Amst)*. 2018;10:196–209.